Polymer Vol. 37 No. 12, pp. 2335–2343, 1996

0032-3861/96/$15.00 + 0.00

Dynamic two-dimensional infra-red spectroscopy of the crystal–amorphous interphase region in low-density polyethylene

Ann Singhal and Leslie J. Fina*
Department of Mechanics and Materials Science, College of Engineering, Busch Campus, Rutgers University, PO Box 909, Piscataway, NJ 08855, USA
(Received 10 June 1995; revised 18 September 1995)

Dynamic two-dimensional Fourier transform infra-red (*FT*i.r.) spectroscopy has been used to study the nature of the interphase in low-density polyethylene (LDPE). A two-dimensional correlation analysis on the dynamic spectra indicates that neat LDPE is comprised of three regions: an ordered crystalline region, a disordered, liquid-like region, and a crystal/amorphous interfacial region. The 1468 cm^{-1} peak in the methylene bending region is assigned to all-*trans* structures which primarily reside in the interfacial region. A variety of LDPE samples with different additives are used in order to determine how the additives influence the dynamic mechanical properties of each morphological phase. It is found that talc associates with the crystallites, ethylene vinyl acetate is distributed in all three morphological phases of the LDPE, and pyrene is associated only with the non-crystalline regions. Copyright © 1996 Elsevier Science Ltd.

(Keywords: two-dimensional *FT*i.r. spectroscopy; step-scan interferometry; low-density polyethylene)

INTRODUCTION

In the past, a limited amount of work has been done in an effort to understand the relationship between the macroscopic properties and the changes occurring at the molecular level during dynamic mechanical deformation. In this present work, an attempt is made to understand the morphology of low-density polyethylene (LDPE) at the molecular level by using two-dimensional step-scan *FT*i.r. spectroscopy. This technique is well suited for providing an insight into the molecular processes where infra-red spectra are collected during the dynamic mechanical perturbation[1–5]. When a polymer sample is dynamic mechanically perturbed, the chemical functional groups on the polymer chains reorient at different rates and have a wide variety of phase relationships to the stretching cycle. While all phase angles occur in a dynamic mechanically stretched polymers, with infra-red spectroscopy the movement of each chemical group can be separated into in-phase (0°) and out-of-phase (90°) responses in the same way as dynamic mechanical analysis is carried out. Furthermore, since in-phase and out-of-phase responses are measured as a function of infra-red wavenumber, it is possible to compare the responses of specific functional groups with each other, as well as to the macroscopic strain.

Polyethylene has a morphological phase structure that is comprised of crystalline and non-crystalline regions. In the crystalline regions, the structure is well known from X-ray diffraction studies. The molecules are straight rods with planar zigzag carbon skeletons, usually organized in an orthorhombic unit cell. This unit cell contains two chains, whose repeat unit consists of two CH_2 groups. The symmetry group of each chain is isomorphic with the point group D_{2h}, as is the factor group of the space group in the unit cell[6–8]. In non-crystalline regions, it is now known that a third phase is present between the crystalline and amorphous phases[9–14], since the boundary between ordered crystalline regions and the disordered non-crystalline regions cannot be sharp. Some of the chains that emanate from the basal plane of the lamellar crystallites return to the same crystallite but not necessarily in juxtaposition. Other chains terminate in the amorphous phase or span multiple crystallites. The transition from well-ordered crystals to random amorphous chains is accompanied by a high chain flux and a highly restricted conformational environment. As a result a diffuse boundary or interphase is formed. A variety of techniques such as ^{13}C nuclear magnetic resonance (n.m.r.) spectroscopy[11], small-angle neutron scattering (SANS)[12], Raman spectroscopy[13] and dielectric relaxation[14] have shown that the interfacial region is a significant component in semi-crystalline polyethylene. The thickness of this interfacial region in linear polyethylene has been determined to be in the range of 13–33 Å, depending largely on the molecular weight of the sample[10]. This is of the order of 7–13 vol%. Increases in the molecular weight have been shown to increase the fraction of interfacial material. In the case of LDPE, the

* To whom correspondence should be addressed

interphase is expected to be a more prominent feature of the morphological structure due to the disturbance of the branch points in the crystals.

In this present study the interfacial region of LDPE is examined directly with two-dimensional (2D)-i.r. spectroscopy. A variety of LDPE samples with different additives are used in order to determine how the additives influence the dynamic mechanical properties of each morphological phase. Additives have been chosen for their potential to reveal new information on the interphase and their spectroscopic distinguishability.

EXPERIMENTAL

Sample preparation

Neat low-density polyetheylene (LDPE) and LDPE with a talc additive (talc at ~ 11%) were provided by a proprietary industrial source. A copolymer of LDPE and ethylene vinyl acetate (3.5 wt%) was provided by the Mobil Chemical Co. To obtain LDPE films containing the organic additive pyrene, LDPE films were soaked in a saturated chloroform solution of pyrene (research grade, obtained from Lancaster Synthesis Ltd) for 3 days at 40°C, and then dried for 2 days in the ambient environment to completely remove the chloroform[15]. All films were 1 ml thick and crystallinities were in the range of 51–63%, as determined by curve-fitting the methylene rocking region of the transmission infra-red spectra. Before scanning, each sample was sanded in order to remove any potential interference fringe effects.

Instrumentation

Details of the experimental set-up can be found elsewhere[1]. All films were approximately 2.5 cm long and 1.5 cm wide. For 2D-i.r. scanning, a 25 mm diameter sapphire low-pass filter with an undersampling ratio of 8 ($4\lambda_{HeNe}$ data spacing per digitization) is used to scan the 1800–400 cm^{-1} region of the polyethylene films. The undersampling is used in order to reduce the acquisition time and the noise level. The spectral resolution is set at 4 cm^{-1} and a step-scan rate of 0.25 Hz is used to collect a total of 16000 signals from each of the three output channels: lock-in 1 (phase insensitive), lock-in 2 (in-phase), and lock-in 2 (quadrature). Eight scans are co-added in order to reduce the noise in the spectra. All the samples are scanned several times, with only the reproducible spectal features being reported here.

RESULTS

Low-density polyethylene

A considerable amount of work has been carried out in the analysis of the methylene bending region in the infra-red spectra of polyethylene and n-alkanes. However, the nature of all of the peaks has not been revealed. It is well known that the two narrow half-width peaks which occur at ~ 1472 and 1462 cm^{-1} result from the crystal field splitting in polyethylene and n-alkane orthorhombic and monoclinic unit cells[16–18]. The peak which occurs at ~ 1455 cm^{-1} has been assigned to methylene bending vibrations in conformationally disordered groups[19,20], while the peak at ~ 1467 cm^{-1} is assigned to bending vibrations in all-*trans* methylene chain sequences outside of the crystal structures[21,22]. Agosti *et al.*[21] point out that the peak position of methylene bending and rocking

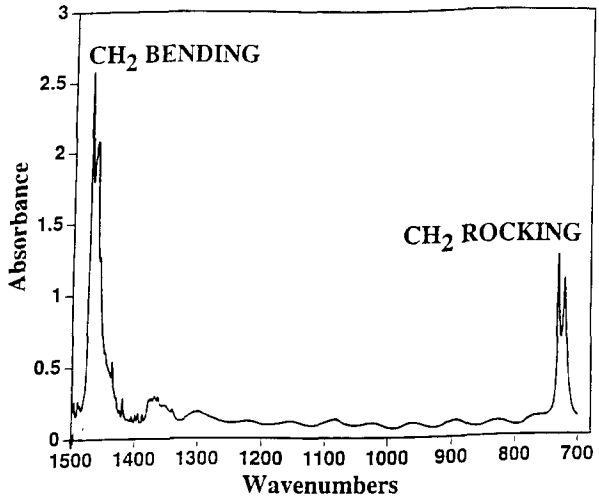

Figure 1 Static infra-red absorbance spectrum of unoriented neat LDPE

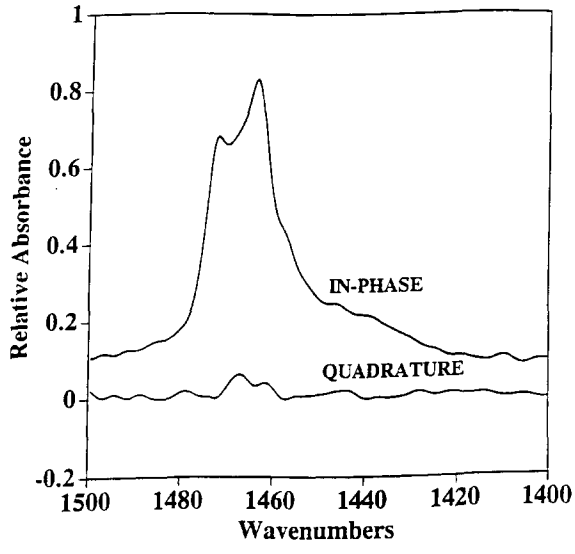

Figure 2 In-phase and quadrature step-scan dynamic spectra of neat LDPE in the CH_2 bending region

modes resulting from all-*trans* sequences occurs approximately in the middle of the crystal-field-split positions when the static potential energy does not shift the centre of mass of the doublet.

Figure 1 shows the CH_2 bending and rocking regions of the conventional absorbance spectrum of as-received neat LDBE. *Figure 2* shows the in-phase and quadrature dynamic step-scan spectra in the CH_2 bending region. The in-phase component of the dynamic spectra is obtained by ratioing the Fourier transform of the in-phase output of the second lock-in amplifier to the sample transmission measured simultaneously from the first lock-in amplifier. The quadrature component of the dynamic infra-red spectra is obtained analogously from the quadrature output of the second lock-in amplifier. The dynamic spectra contain only the changes in the absorption due to the application of the mechanical perturbation. From the dynamic spectra it can be observed that the response in the quadrature spectrum is small relative to that in the in-phase spectrum, which shows that the polymer film

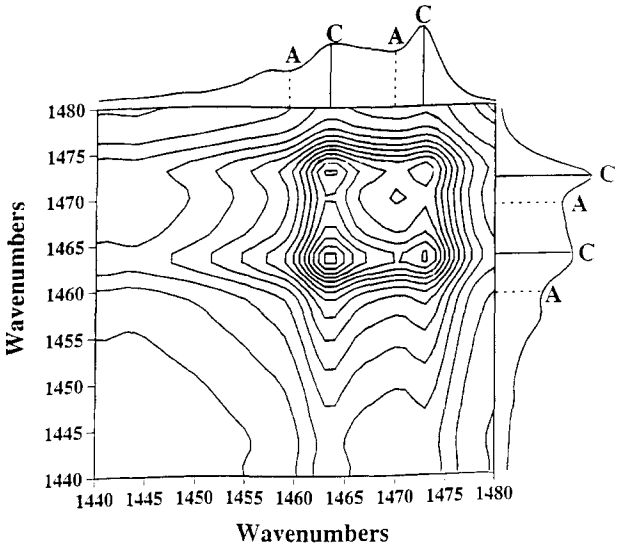

Figure 3 2D-*FT*i.r. synchronous correlation plot of neat LDPE in the CH_2 bending region

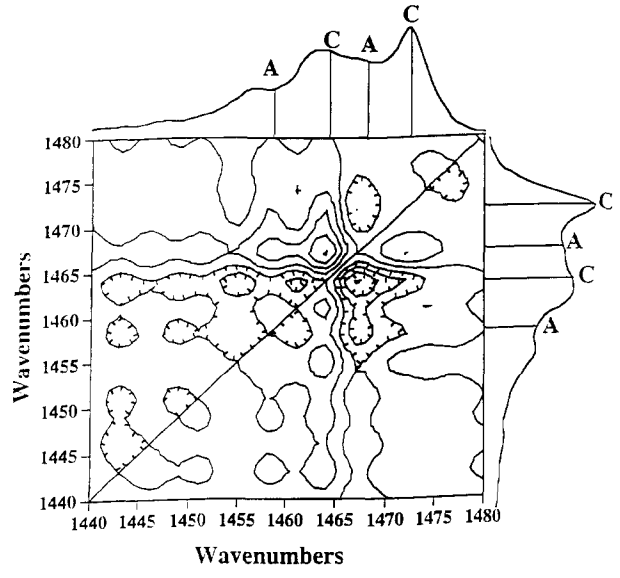

Figure 4 2D-*FT*i.r. asynchronous correlation plot of neat LDPE in the CH_2 bending region

in this region responds mostly in-phase with the applied strain. The in-phase spectrum in the CH_2 bending region is similar to the normal absorbance spectrum. The in-phase and quadrature spectra can be used to generate synchronous and asynchronous correlation plots[2]. In the synchronous plot, the autopeaks observed along the diagonal indicate that these absorbances change as a result of the external perturbation applied to the polymer film and the crosspeaks observed at off-diagonal positions indicate infra-red features that are dynamically changing in-phase with each other. On the other hand, in the asynchronous plot, off-diagonal crosspeaks connect infra-red features that are changing out-of-phase with each other. More information on the theory and basis for a correlation analysis can be found elsewhere[3,4]. *Figure 3* shows the synchronous correlation plot of the CH_2 bending region generated from the dynamic infra-red spectra shown in *Figure 2*. The

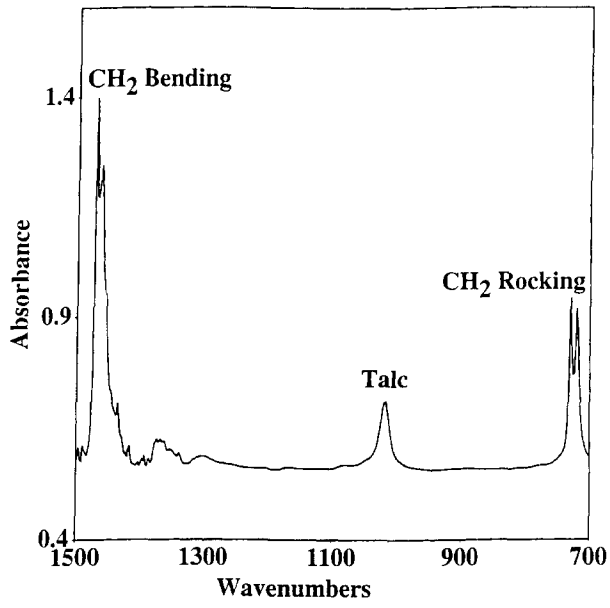

Figure 5 Static absorbance spectrum of LDPE with a talc additive

synchronous plot shows strong autopeaks at 1464 and 1472 cm^{-1}. Intense autopeaks typify crystalline species in semicrystalline polymers. The presence of the crosspeaks between the two peaks implies that the dynamic strain results in the components moving in-phase with each other as expected from their equivalent morphological origin. *Figure 4* shows the asynchronous plot in the same region. The composite nature of the CH_2 bending region is well demonstrated by this plot, which shows that the 1455 to 1475 cm^{-1} region splits into at least four independent components, at 1458, 1462, 1467, and 1472 cm^{-1}. Analysis of the crosspeaks shows that the two bands at 1464 and 1472 cm^{-1} are out-of-phase with the bands at 1458 and 1467 cm^{-1}. In addition, the component associated with the 1458 cm^{-1} peak is responding at a different rate than the component associated with the band at 1467 cm^{-1}, i.e. a cross-peak is present. The latter is evidence for two mechanically separate disordered phases.

LDPE with a talc additive

The normal absorbance spectrum of LDPE with talc (~ 11%) shown in *Figure 5* has one prominent talc peak at 1020 cm^{-1}. The dynamic spectra in the CH_2 bending region are found to be very similar to that of neat LDPE and are therefore not shown. *Figure 6* shows the synchronous plot of the 1020 cm^{-1} talc region. The strong autopeak observed at ~ 1020 cm^{-1} is evidence that the talc crystals are responding strongly to the applied strain. *Figure 7* shows the synchronous crossplot between the talc region and the CH_2 bending region of the LDPE. It is observed that the main talc band at ~ 1020 cm^{-1} shows strong crosspeaks with the bands at 1464 and 1472 cm^{-1} of the CH_2 bending region. The corresponding intensities in the asynchronous plot (not shown) are very weak.

LDPE–ethylene vinyl acetate (LDPE–EVA) copolymer

Figure 8 shows the normal absorbance spectrum of an LDPE–EVA copolymer with an EVA content of

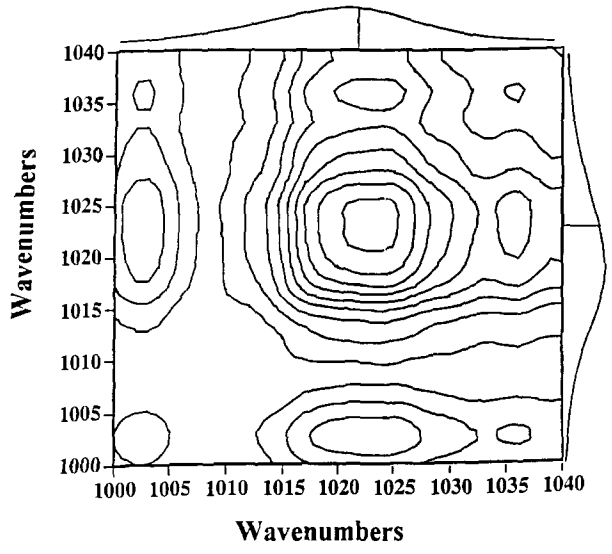

Figure 6 2D-*FT*i.r. synchronous correlation plot of LDPE with talc additive in the talc region

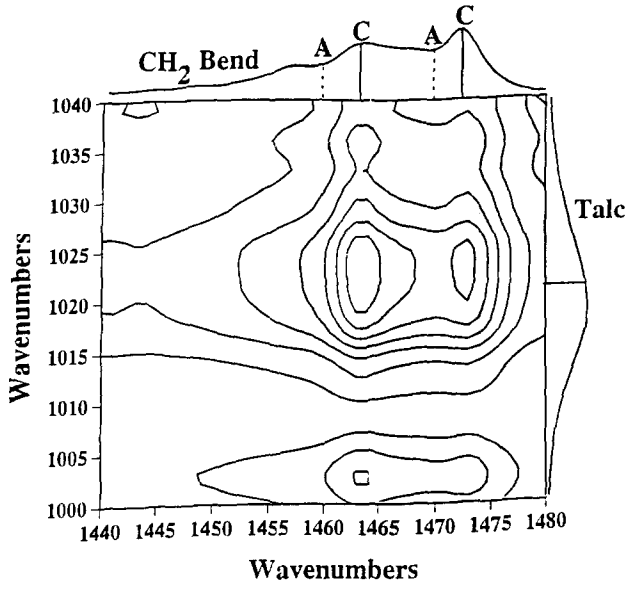

Figure 7 2D-*FT*i.r. synchronous correlation crossplot between the CH_2 bending region of LDPE and the talc region

3.5 wt%. Bands due to EVA are observed at 1740 (C=O stretching), 1370 (symmetrical deformation of the CH_3 groups), 1240 (skeleton O=C–O–C), and 1020 cm^{-1} (skeleton C–O–C). The dynamic spectra of this system in the methylene bending region are again very similar to that of the neat LDPE dynamic spectra and are therefore not shown. The 1740 cm^{-1} peak of the EVA comonomer is correlated with the ethylene sequences of LDPE in the CH_2 bending region. The self-correlation plots of the EVA carbonyl peak are shown in *Figures 9* and *10*. *Figure 9* shows a strong autopeak at 1740 cm^{-1} in the synchronous plot, while the asynchronous plot in *Figure 10* shows that the autopeak at 1740 cm^{-1} splits into three peaks at 1738, 1742, and 1746 cm^{-1}. Analysis of the crosspeaks in the asynchronous plot shows that the main peak at 1742 cm^{-1} is out-of-phase with the two other bands at 1738 and 1746 cm^{-1}. *Figures 11* and *12* show, respectively, the synchronous and the asynchronous crossplots between the C=O stretching region of the

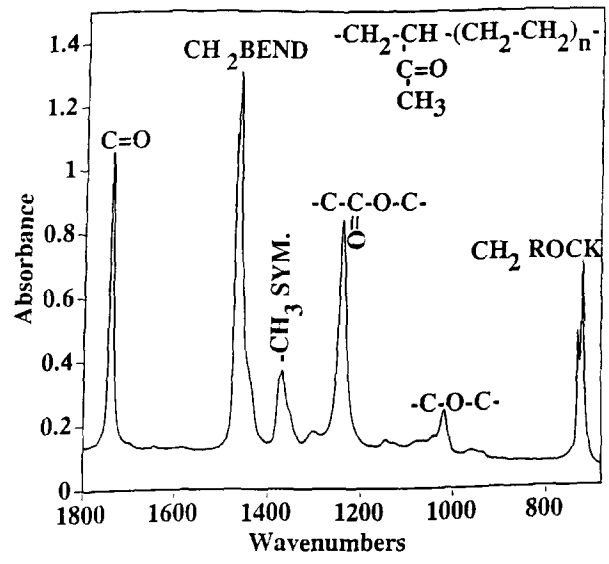

Figure 8 Static absorbance spectrum of the LDPE–EVA copolymer

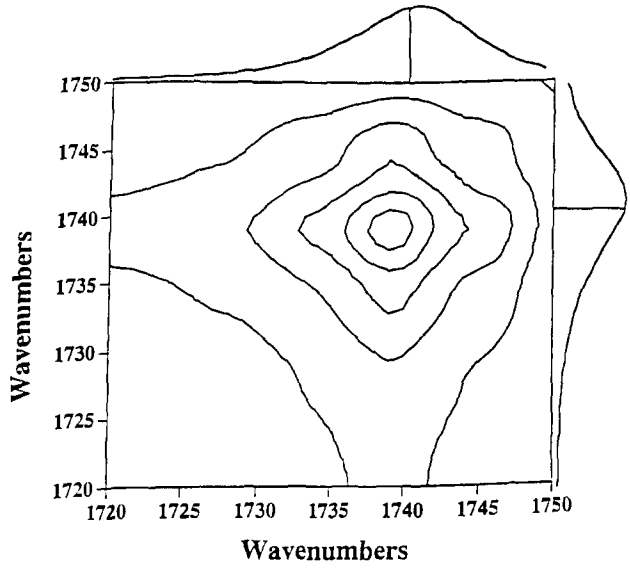

Figure 9 2D-*FT*i.r. synchronous correlation plot of the LDPE–EVA copolymer in the C=O stretching region

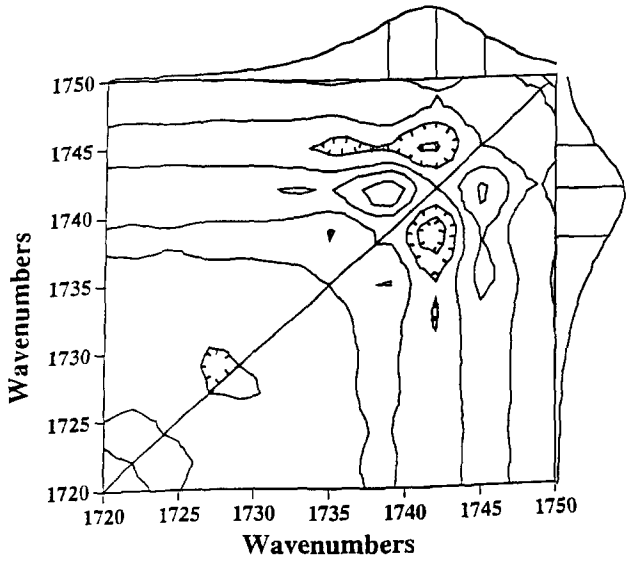

Figure 10 2D-*FT*i.r. asynchronous correlation plot of the LDPE–EVA copolymer in the C=O stretching region

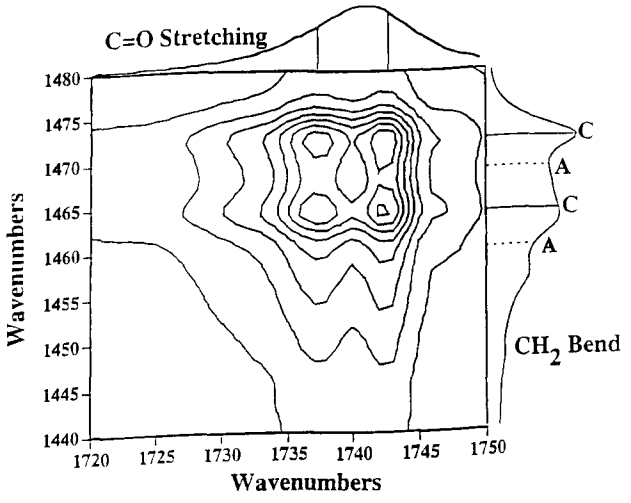

Figure 11 2D-*FT*i.r. synchronous correlation crossplot between the CH_2 bending region and C=O stretching region of the LDPE–EVA copolymer

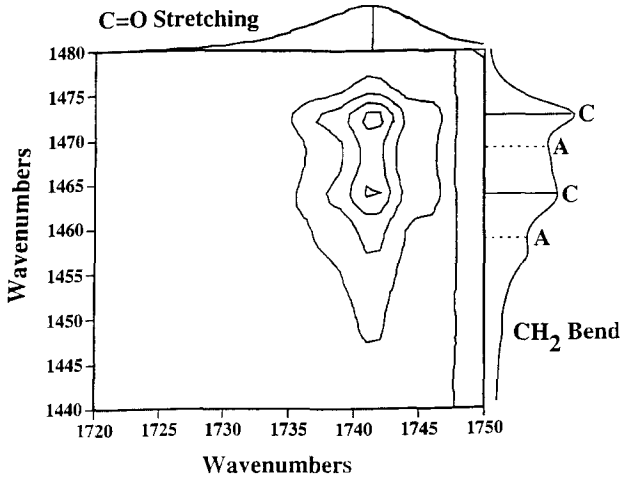

Figure 12 2D-*FT*i.r. asynchronous correlation crossplot between the CH_2 bending region and C=O stretching region of the LDPE–EVA copolymer

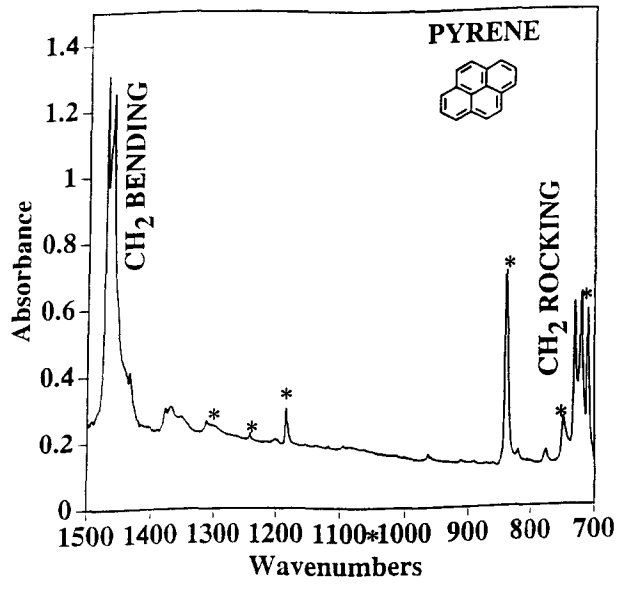

Figure 13 Static absorbance spectrum of LDPE absorbed with pyrene

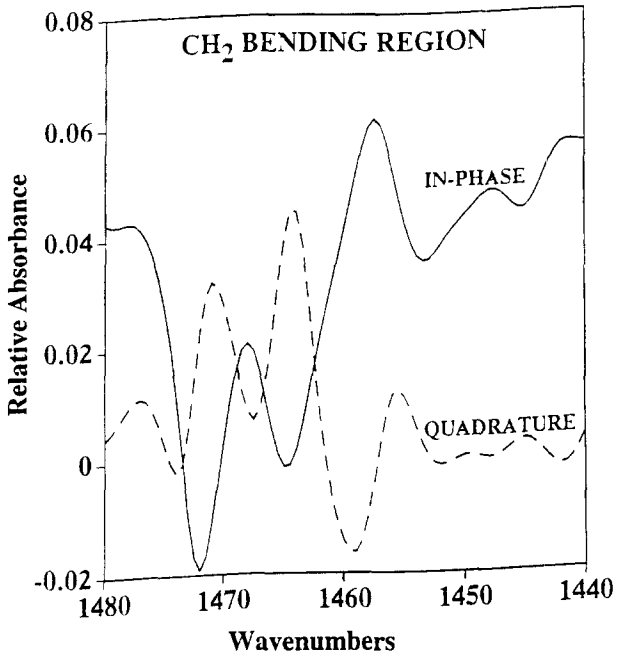

Figure 14 In-phase and quadrature step-scan dynamic spectra in the CH_2 bending region of LDPE absorbed with pyrene

EVA and the CH_2 bending region of LDPE. It can be seen that the two components at 1738 and 1746 cm^{-1} of the C=O stretching region are in-phase, while the third component at 1742 cm^{-1} is out-of-phase with the two bands at 1464 and 1472 cm^{-1} of the CH_2 bending region. Further discussion of these features is presented later.

LDPE with pyrene

Figure 13 shows the normal absorbance spectrum of the LDPE film with pyrene adsorbed into the film, where all of the peaks marked with an asterisk are due to pyrene; the film has ~ 14 wt% absorbed pyrene. Absorption of pyrene into the film produces no detectable changes in the static absorbance spectra of the CH_2 bending and CH_2 rocking regions of the LDPE, suggesting that the crystallinity remains the same, a point also supported by curve-fitting of the CH_2 rocking region. *Figure 14* shows the dynamic spectra of the CH_2 bending region of the sample. A very different behaviour is observed when compared with earlier figures, i.e. a large response is observed in the quadrature. Unlike the neat LDPE material, LDPE with talc and the LDPE–EVA copolymer, the introduction of pyrene changes the deformation mechanism of all of the morphological components in the LDPE. The band from pyrene at ~ 837 cm^{-1} is correlated with the CH_2 bending region of the LDPE in this present work. *Figures 15* and *16* show, respectively, the synchronous and asynchronous crossplots between the pyrene band and the CH_2 bending region. In the synchronous plot (*Figure 15*) the pyrene band shows a strong crosspeak with the 1467 cm^{-1} band of the LDPE and a weak crosspeak with the 1458 cm^{-1} band of the LDPE. On the other hand, the pyrene band shows a crosspeak with the two bands at 1464 and 1472 cm^{-1} of the CH_2 bending region in the asynchronous plot.

DISCUSSION

It is well known that the doublet observed in the infrared spectrum of LDPE in the CH_2 bending region at

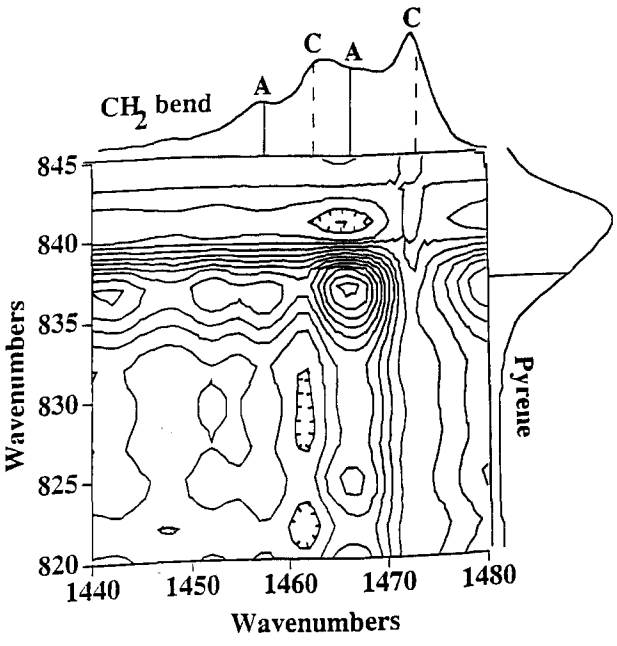

Figure 15 2D-*FT*i.r. synchronous correlation crossplot between the CH_2 bending region and the pyrene region of LDPE absorbed with pyrene

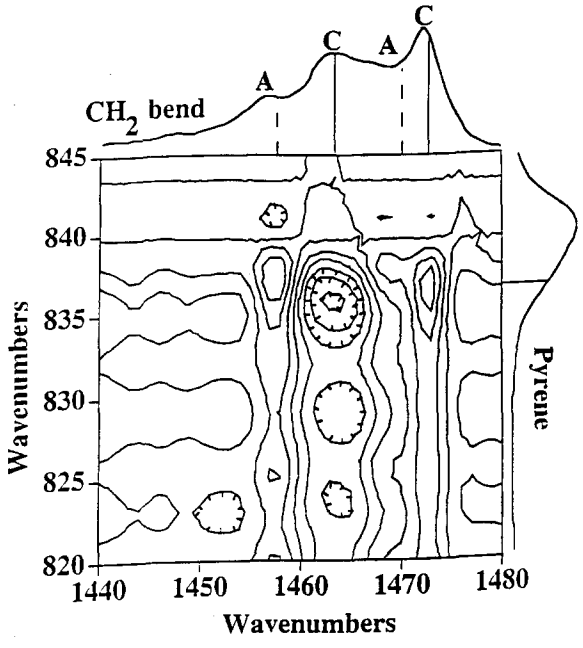

Figure 16 2D-*FT*i.r. asynchronous correlation crossplot between the CH_2 bending region and the pyrene region of LDPE absorbed with pyrene

1464 and 1472 cm^{-1} originates from a factor group splitting due to the packaging of two polymer chains in the unit cell of an orthorhombic lattice[6–8]. This leads to the crystalline assignment of these two peaks and is consistent with the fact that both the bands respond strongly to the applied strain and are in-phase with each other in the synchronous plot (*Figure 3*). Furthermore, the presence of asynchronous crosspeaks between the crystalline bands (1464 and 1472 cm^{-1}) and the band at 1467 cm^{-1} (*Figure 4*) suggests that the 1467 cm^{-1} band has primarily a non-crystalline origin. The particularly interesting feature that is apparent in *Figure 4* is the out-of-phase relationship of the two non-crystalline bands, which suggests that they have a different morphological origin. This conclusion is in agreement with earlier work, where the 1458 cm^{-1} band is assigned to the amorphous regions comprised mostly of *gauche* conformations of methylene segments, and the 1467 cm^{-1} band is assigned to methylene bending modes organized in fully transplanar segments in the interphase region[21]. Therefore, neat LDPE is comprised of three regions: an ordered crystalline region, a disordered, liquid-like region, and an interfacial region. This model is shown schematically in *Figure 17a*.

The addition of talc to LDPE produces no detectable changes in the CH_2 bending region of LDPE in both the normal 'static' absorbance spectrum and the dynamic spectra. This implies that the talc does not change the dynamic deformation mechanism of the LDPE. However, other evidence suggests that talc increases the static flexural and tensile moduli and the heat deflection temperature[23]. The presence of strong synchronous crosspeaks between the crystalline bands of the CH_2 bending region and the main talc peak (*Figure 7*) suggests that the talc is in intimate association with the crystallites and not closely associated with the non-crystalline phases. This is shown schematically in *Figure 17b*. In polymer applications, talc crystals are generally in the form of platelets with an average diameter of $\sim 10\,\mu m$[24]. It is also known that when talc is added during polyethylene processing, it acts as a nucleating agent for crystal growth. Nonetheless, the dynamic deformation of the LDPE crystallites is not disturbed by the presence of talc. In addition, the presence of talc does not change the dynamic deformation of the amorphous or interphase material, as the same set of crosspeaks are observed in the asynchronous plot of the CH_2 bending region in LDPE with talc (figure not shown) as in the corresponding plot of neat LDPE (*Figure 4*).

In the LDPE–EVA copolymer, it is observed that the C=O stretching band of EVA has three different components under it, one of which responds strongly to the external perturbation (1740 cm^{-1}) and is out-of-phase with the other two components at 1738 and 1746 cm^{-1} (*Figures 9* and *10*). The synchronous and asynchronous crossplots between the C=O stretching vibration and the CH_2 bending show that the EVA is both in-phase and out-of-phase with the two crystalline bands at 1464 and 1472 cm^{-1} of the LDPE bending region (*Figures 11* and *12*). In the asynchronous plot of the methylene bending region in this material (not shown), the interphase band at 1467 cm^{-1} is *not* out-of-phase with the amorphous band at 1458 cm^{-1}, as is the case in the previously discussed samples, although both bands remain out-of-phase with the crystalline bands. Therefore, the presence of the EVA comonomer alters the mechanical relationship between the 'true' amorphous phase and the interphase from that observed in neat LDPE and LDPE with talc. The picture that develops from this data is that EVA is associated with both the crystalline and non-crystalline regions (including both interfacial and amorphous regions). The distribution of EVA is depicted schematically in *Figure 17c*, and is believed to be present in the crystals as defects, on the surface of the crystals and in the amorphous phase. However, this distribution of EVA

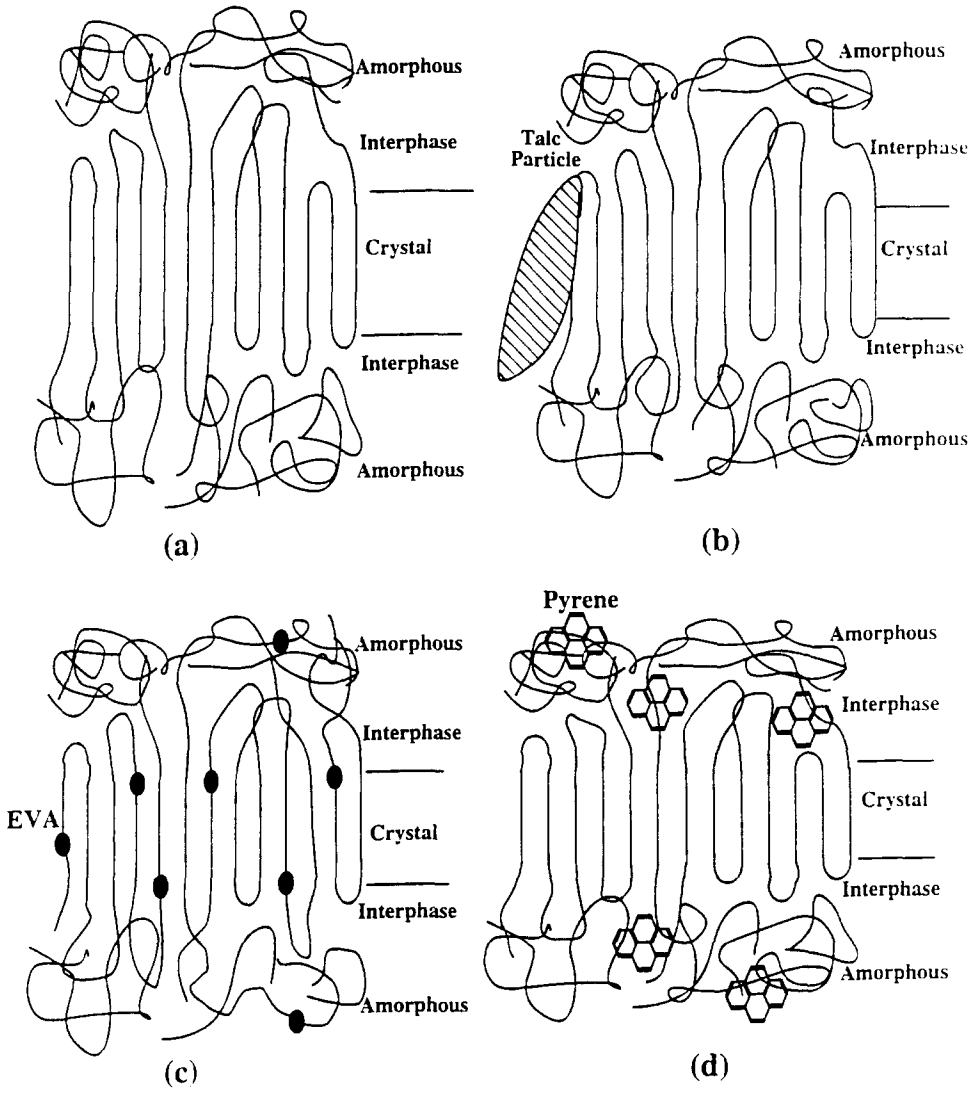

Figure 17 Schematic structure models proposed for LDPE with various additives, showing crystalline, interfacial, and amorphous regions: (a) neat LDPE; (b) LDPE with talc additive; (c) LDPE–EVA copolymer (3.5 wt% EVA), where circles represent EVA monomers; (d) LDPE with pyrene

does not have large effects on the deformation mechanism, since the dynamic spectra are very similar to that of neat LDPE.

When pyrene is introduced into LDPE, a very different dynamic behaviour is observed. A large response in the quadrature occurs and the in-phase spectrum is very different from that of neat LDPE. The addition of pyrene significantly changes the deformation mechanism of all of the morphological phases in LDPE. The presence of synchronous crosspeaks between the pyrene band at 837 cm^{-1} and the two non-crystalline bands (1458 and 1467 cm^{-1}) (*Figure 15*), and the asynchronous crosspeaks of the 837 cm^{-1} band with the two crystalline bands at 1462 and 1474 cm^{-1} (*Figure 16*), indicates that the pyrene is moving in-phase with both of the non-crystalline components and out-of-phase with the crystalline regions of the LDPE. These results suggest that pyrene is excluded from the LDPE crystallites and is present in both of the non-crystalline phases of the LDPE. This conclusion is corroborated by the work carried out on the adsorption of pyrene and other similar aromatic organic molecules in LDPE[25–27], where it was suggested that organic molecules reside in the non-crystalline regions of LDPE. A schematic representation of this morphological model of LDPE with absorbed pyrene is shown in *Figure 17d*. The adsorption of pyrene molecules into the interphase and amorphous region is responsible for the alteration of the deformation behaviour of the crystallites, where a significant phase-lag behind the applied strain occurs.

The in-phase and quadrature spectra are also used to calculate the phase angle β, which is related to the time delay of the spectral changes occurring at a certain wavenumber resulting from an external perturbation. The magnitude of these spectral changes is represented by the power spectrum, which shows the system's susceptibility to the applied strain, i.e. a larger response of the infra-red feature to the applied strain leads to a higher intensity in the power spectrum for that functional group or the microstructural component. If $IQ(\nu)$ represents the quadrature spectrum and $IP(\nu)$ the in-phase spectrum, then:

$$\beta(\nu) = \arctan\left[IQ(\nu)/IP(\nu)\right] \quad (1)$$

$$P(\nu) = \left[IQ(\nu)^2 + IP(\nu)^2\right]^{1/2} \quad (2)$$

where $\beta(\nu)$ is the phase spectrum and $P(\nu)$ is the power spectrum. Further information on this theory can be

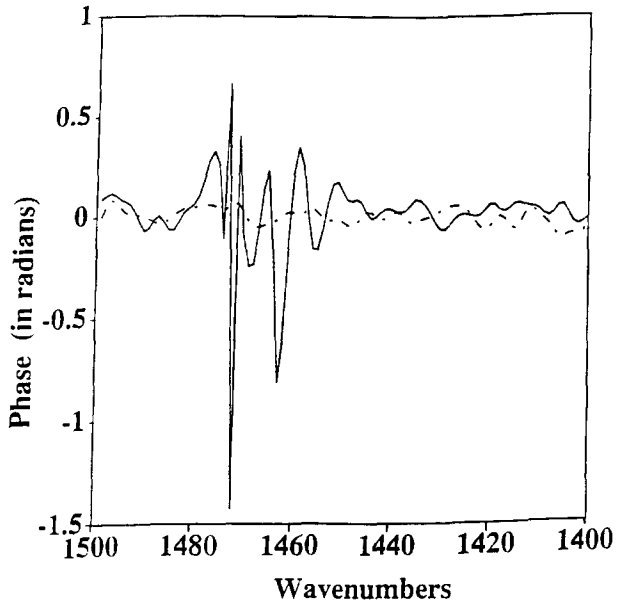

Figure 18 Phase spectra of the neat LDPE (dashed line) and LDPE absorbed with pyrene in the CH_2 bending region of LDPE

obtained elsewhere[28,29]. *Figure 18* shows the phase spectrum of neat LDPE and LDPE with pyrene in the CH_2 bending region of the LDPE. The phase spectrum of LDPE shows that the response of all morphological phases in this region is mostly in-phase with the applied strain (dashed line). In LDPE with pyrene, the phase changes rapidly across the crystalline bands at 1462 and 1474 cm^{-1} and reaches a phase-delay of 90° with respect to the applied strain. This further supports the conclusion that the absorption of pyrene substantially alters the deformation mechanism of LDPE.

An absorption band at 1467 cm^{-1} has been seen experimentally in isotopic dilution studies of polyethylene[30]. This suggests that the 1467 cm^{-1} band observed in this present study in the normal and dynamic spectra of the LDPE is in fact resulting from the all-*trans* methylene segments protruding from the crystalline lamella forming the interphase. A band at 1468 cm^{-1} has also been seen in the micellular phase of sodium laurate, sodium oleate and α,ω-d_5 sodium laurate, and the liquid crystal phase of lipids[31]. Due to the different conformational and morphological origins of the two bands at 1467 and 1458 cm^{-1}, an asynchronous cross-peak occurs between these two bands in the CH_2 bending region of neat LDPE (*Figure 4*). In order to verify that the 1467 cm^{-1} peak results from all-*trans* methylene segments in the interphase, relative crystallinites are calculated by curve-fitting the CH_2 rocking and bending regions of neat LDPE and LDPE with various additives. The data for the rocking region is shown in column A of *Table 1*. The crystallinity obtained by curve-fitting the CH_2 bending region, including the contribution from the interphase represented by the band at 1467 cm^{-1} as a crystalline component, is calculated in the following way:

$$\text{Crystallinity} = \frac{I(1472 + 1467 + 1462)}{I(1472 + 1467 + 1462 + 1458 + 1440)} \times 100 \quad (3)$$

where I represents the observed infra-red intensities for the band indicated. The data obtained by curve-fitting neat LDPE and LDPE with various additives for the CH_2 bending region is shown in column B of *Table 1*. On comparison of columns A and B of *Table 1* one can see that the values are in excellent agreement, particularly for the first three samples. This observation is consistent with the fact that in the infra-red spectra of molten and glassy polyethylenes and n-alkanes[17], the CH_2 sequences that are all-*trans* have peak frequencies close to that of the lower-frequency peak of the methylene rocking crystal field splitting and have relatively narrow half-widths[17,18]. The peak from the all-*trans* methylene rocking modes in the interphase is heavily overlapped with the crystal peak. This implies that the calculation of crystallinity by curve-fitting of the CH_2 rocking region with three peaks leads to the inclusion of interphase material as crystalline species. In columns C–E of *Table 1* the relative amounts of each of the three phases as found from the bending region are shown. It is noted that no consideration of different crystal/amorphous/interphase absorption coefficients is used in the bending region, which would slightly change the reported values.

CONCLUSIONS

A two-dimensional correlational analysis on the dynamic two-dimensional infra-red spectra of neat LDPE shows that the CH_2 bending region is comprised of a crystalline phase represented by the bands at 1472 and 1462 cm^{-1}, an interphase region represented by the band at 1467 cm^{-1} and a liquid-like isotropic amorphous phase represented by the bands at 1458, 1450, and 1440 cm^{-1}. The band representing the interphase at 1467 cm^{-1} is found to be from the all-*trans* methylene segments protruding from the crystalline lamella. The addition of talc and ethylene vinyl acetate to LDPE does not change the dynamic deformation mechanism of the

Table 1 Comparison of relative crystallinities for neat LDPE and LDPE with various additives, calculated from the CH_2 rocking (A) and CH_2 bending regions (B–E)

Sample	Crystallinity from CH_2 rocking region, A[a](%)	Crystallinity from CH_2 bending region (%)			
		B[b]	C[c]	% Interphase, D[c]	% Amorphous, E[c]
Neat LDPE	51	53	27	41	32
LDPE with talc	61	60	33	28	39
LDPE with EVA	63	64	32	32	36
LDPE with pyrene	54	66	43	28	29

[a] Using an adsorption coefficient ratio (crystal/amorphous) of 1.20 (ref. 20)
[b] Calculation with the 1467 cm^{-1} peak as part of the crystalline phase
[c] Calculation of the 1467 cm^{-1} peak as part of the crystal/amorphous interphase

LDPE but their morphological distribution in LDPE is found to be very different. Talc associates intimately with the crystallites and EVA associates with all three of the morphological phases (crystalline, interphase, and amorphous). On the other hand, absorption of pyrene changes the deformation mechanism of all of the morphological phases in LDPE, being excluded from the LDPE crystallites and associated with both of the non-crystalline phases.

REFERENCES

1 Singhal, A. and Fina, L. J. *Appl. Spectrosc.* in press
2 Noda, I., Dowery, A. E. and Marcott, C. *Appl. Spectrosc.* 1988, **42,** 203
3 Noda, I. *Appl. Spectrosc.* 1990, **44,** 550
4 Marcott, C., Dowery, A. E. and Noda, I. *Appl. Spectrosc.* 1993, **47,** 1324
5 Noda, I. *Appl. Spectrosc.* 1993, **47,** 1239
6 Tasumi, M. and Shimanouchi, T. *J. Chem. Phys.* 1965, **43,** 1245
7 Nielsen, J. R. and Holland, R. F. *J. Mol. Spectrosc.* 1961, **6,** 394
8 Tobin, M. C. and Carrano, M. J. *J. Chem. Phys.* 1956, **25,** 1044
9 Flory, P. J., Yoon, D. Y. and Dill, K. A. *Macromolecules* 1984, **17,** 862
10 Mandelkern, L., Alamo, R. G. and Kennedy, M. A. *Macromolecules* 1990, **23,** 4721
11 Kitamaru, R. and Horii, F. *Adv. Polym. Sci.* 1977, **16,** 137
12 Russel, T. P., Ito, H. and Wignall, G. D. *Macromolecules* 1988, **21,** 1703
13 Strobl, G. R. and Hagedorn, W. *J. Polym. Sci. Polym. Phys. Edn.* 1978, **16,** 1181
14 Popli, R., Glotin, M. and Mandelkern, L. *J. Polym. Sci. Polym. Phys. Edn.* 1984, **22,** 448
15 Radziszewski, J. G. and Michl, J. *J. Phys. Chem.* 1981, **85,** 2934
16 Krimm, S. C., Lang, Y. and Sutherland, G. B. B. M. *J. Chem. Phys.* 1956, **25,** 1316
17 Snyder, R. G. *J. Chem. Phys.* 1967, **47,** 1316
18 Hagemann, H., Strauss, H. L. and Snyder, R. G. *Macromolecules* 1987, **20,** 2810
19 Zerbi, G., Gallino, G., Fanti, N. D. and Baini, L. *Polymer* 1989, **30,** 2324
20 Hagemann, H., Snyder, R. G., Peacock, A. J. and Mandelkern, L. *Macromolecules* 1989, **22,** 3600
21 Agosti, E., Zerbi, G. and Ward, I. M. *Polymer* 1992, **33,** 4219
22 Hübner, W., Wong, P. T. T. and Mantsch, H. H. *Biochem. Biophys. Acta* 1990, **1027,** 229
23 'Chemical Additives for the Plastics Industry', Noyes Data Corporation, Radian Corporation, 1987
24 Darlington, M. W. and Nascimento, R. S. V. in Proceedings of the Joint Conference of the Plastics and Rubber Institute and the British Plastics Federation, Elsevier, Barking, Essex, 1986, p. 15/1
25 Phillips, P. J. *Chem. Rev.* 1990, **90,** 425
26 Jang, Y. T. and Phillips, P. J. *J. Polym. Sci. Polym. Phys. Edn.* 1986, **24,** 1259
27 Jang, Y. T., Phillips, P. J. and Thulstrup, E. W. *Chem. Phys. Lett.* 1982, **93,** 66
28 Budevska, B. O., Christopher, J. M., Griffiths, P. R. and Roginski, R. T. *Appl. Spectrosc.* 1993, **47,** 1843
29 Budevska, B. O., Christopher, J. M. and Griffiths, P. R. *Appl. Spectrosc.* 1994, **48,** 1556
30 Snyder, R. G.and Poore, M. W. *Macromolecules* 1973, **5,** 708
31 Cameron, D. G., Umemura, J., Wong, P. T. T. and Mantsch, H. H. *Colloid Surf.* 1982, **4,** 131

APPENDIX

Note in response to comments from a referee

The authors are grateful to one of the referees who stated that a consideration of the influence of thickness changes on the reported results would be helpful, particularly in light of the fact that (1) a static polarizer was used in the experiments and (2) absorbance changes due to changes in the thickness can be of the same order of magnitude as the absorbance changes due to dipole reorientation. To address this point, an experiment was repeated with neat LDPE using a triple modulation–demodulation setup which included a ZnSe photoelastic modulator operating at 37 kHz and a MCT detector. The net effect of using polarization modulation in the *FT*i.r. dynamic stretching experiment is a subtraction of the parallel and perpendicular polarization components. Therefore, thickness changes are expected to be minimized. All of the features reported herein are reproducible in the triple modulation experiment.